



# Composition and toxicity of particulate matter emitted from turbocharged common rail DME–biodiesel engine

Chunhua Sun<sup>1</sup> · Xinqi Qiao<sup>1</sup> · Dehao Ju<sup>1</sup> · Qing Tang<sup>1</sup> · Xiaoyuan Fang<sup>1</sup> · Feng Zhou<sup>2</sup>

Received: 4 November 2019 / Accepted: 7 January 2020 / Published online: 16 January 2020  
© Springer-Verlag GmbH Germany, part of Springer Nature 2020

## Abstract

Both ultrafine particle and toxicity emissions originating from diesel engine gain an increasing concern. In this study, size distribution and toxicity of particles from a turbocharged common rail engine fueled with *clean fuels*—dimethyl ether (DME) and biodiesel blends—were investigated. Effects of different DME–biodiesel blends (B0, B5, B10, and B15) and different engine loads were considered. The results demonstrate that particles emitted from DME–biodiesel engine are mainly in form of nucleation mode. Engine running at intermediate load exhausts the maximum number of accumulation mode particles owing to local hypoxia and not high enough combustion temperature. The addition of biodiesel slightly increases the total particle number, peak of particle number concentration, and particle size corresponding to the peak. Effect of biodiesel proportion on particle size distribution gets weaker with the increase of engine load. Engine fueled with B5, B10, and B15 mainly exhausts low molecular weight polycyclic aromatic hydrocarbons (PAHs) (ring number  $\leq 4$ ) which are closely related to unburned fuel, and the total PAH emissions are linear versus the fuel consumption. Toxicity equivalent (TE) of particles at low load is lower than that at intermediate load. DME–biodiesel blends with biodiesel mass proportion  $\leq 15\%$  can release the DME engine from abrasion and leakage, but no obvious increase in both particle emissions and the risk of particle toxicity.

**Keywords** Dimethyl ether · Biodiesel · Engine · Particle · Polycyclic aromatic hydrocarbon

## Nomenclature

ATDC	Start of injection timing ( $^{\circ}\text{CA}$ )	DME	Dimethyl ether
B0	100% DME	$D_p$	Particle diameter (nm)
B5	95% DME + 5% biodiesel	EBSFC	Equivalent brake-specific fuel consumption (g/kWh)
B10	90% DME + 10% biodiesel	EGR	Exhaust gas recirculation
B15	85% DME + 15% biodiesel	HC	Hydrocarbon
BMEP	Brake mean effective pressure (MPa)	HRR	Heat release rate ( $\text{J}/^{\circ}\text{CA}$ )
BSFC	Brake-specific fuel consumption (g/kWh)	MPRR	Maximum cylinder pressure rising rate ( $\text{MPa}/^{\circ}\text{CA}$ )
BTE	Brake thermal efficiency	$n$	Speed (rpm)
$\text{CA}_{50}$	Crank angle position for 50% burned mass fraction ( $^{\circ}\text{CA}$ ATDC)	$\text{NO}_x$	Nitrogen oxide
CO	Carbon monoxide	$p$	In-cylinder pressure (MPa)
		PAH	Polycyclic aromatic hydrocarbon
		$P_{\text{inj}}$	Injection pressure (MPa)
		SOI	Start of injection timing ( $^{\circ}\text{CA}$ )
		tr	Temperature of exhaust gas ( $^{\circ}\text{C}$ )

Responsible editor: Philippe Garrigues

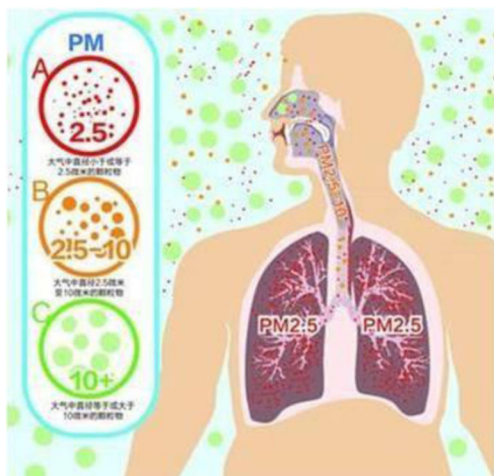
✉ Xinqi Qiao  
qiaoxinqi@sjtu.edu.cn

<sup>1</sup> Key Laboratory of Power Machinery and Engineering, Ministry of Education, Shanghai Jiao Tong University, Shanghai 200240, China

<sup>2</sup> Zhejiang Marine Development Research Institute, Zhoushan 316000, Zhejiang, China

## Introduction

With tightening of petroleum supplies, increasing stringent emission regulations, and challenge from the rising of electric engine demand, there is reduction of the dependence of



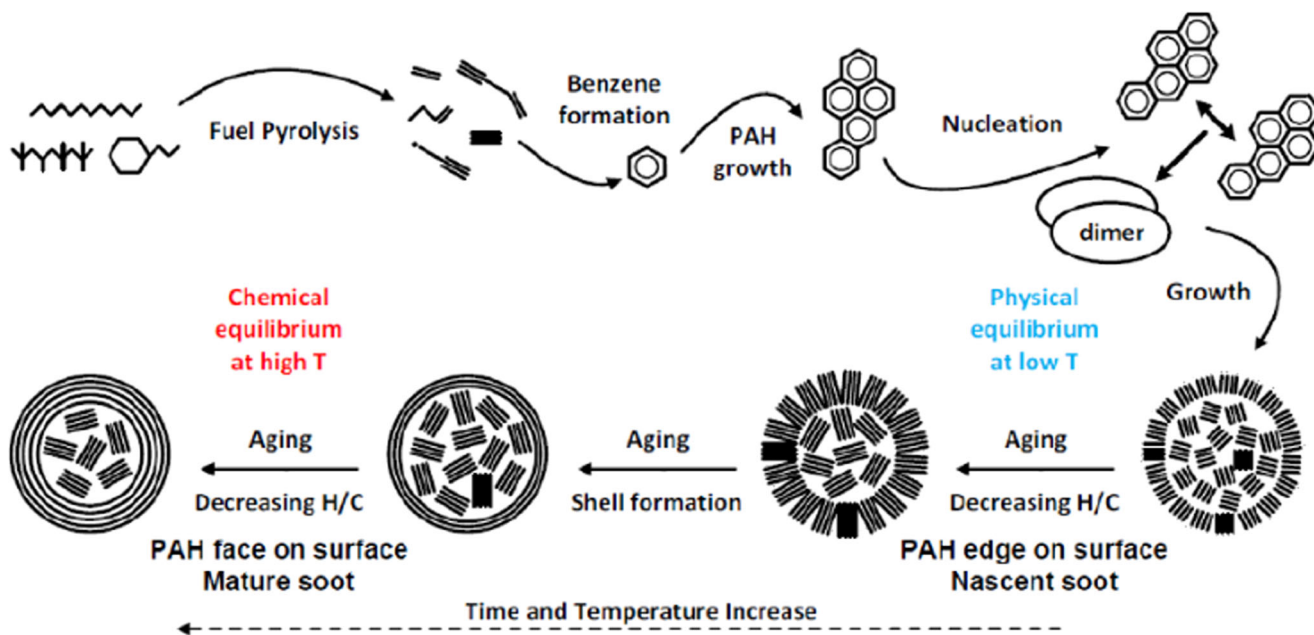
**Fig. 1** Distribution of different size particles in the human respiratory system ([http://www.sohu.com/a/227423041\\_390159](http://www.sohu.com/a/227423041_390159))

internal combustion engine on fossil diesel, thereby operating with low emissions (Şen et al. 2018; Geng et al. 2016). Alternative fuels, such as dimethyl ether (DME) (Benajes et al. 2018), alcohol (Ghadikolaei et al. 2018), methanol (Soni and Gupta 2017), and biodiesel (Musthafa et al. 2018), offer potential to meet the above demands and have been attracting continuing interests. Among various alternative fuels, DME is attractive due to its following properties: oxygen content, no C–C bond, low boiling point, and high cetane number (Lamani et al. 2017; Peng et al. 2017). However, DME is also accompanied by a few unfavorable physical properties such as small bulk modulus, low calorific value, and low viscosity. The small bulk modulus and low viscosity of DME result in higher pressure, violent pressure fluctuation, and vapor leakage in the fuel supply system (high pressure

pump, common rail, and injector) (Cipolat 2007; Cipolat and Bhana 2009). The properties of superior lubricity and high calorific value of biodiesel complement those of DME, and the use of lubrication additives in DME engine can be eliminated by blending biodiesel.

Detailed dynamic, fuel economic performances, and emission characteristics of engine fueled with DME, biodiesel, DME–diesel blend, and biodiesel–diesel blend have been conducted by previous studies, and both benefits and shortages have been indicated. Numerous works have demonstrated that engine fueled with DME or DME blend could achieve almost smoke-free combustion, lower combustion noise, and lower nitrogen oxide ( $NO_x$ ) emissions (Wang et al. 2008). Engine fueled with biodiesel or biodiesel blend can be a benefit for reduction of greenhouse gas emissions and resource reutilization without any hardware modification (Di et al. 2009). The disadvantages of engines fueled with DME or biodiesel include the following: DME engine presents problems such as low combustion enthalpy, low viscosity, poor lubricity, and its adverse reaction to rubber, which necessitate that the fuel supply system be modified (Song et al. 2004). Biodiesel engine presents problems regarding cold starts and an increase in  $NO_x$  emissions (Peng et al. 2017).

The previous works explored the possibility of overcoming the disadvantages and strengthening the advantages of DME and biodiesel by blending them and utilizing their complementary properties. Hyun and Oguma (2002) first conducted research on the spray and exhaust emissions of a diesel engine operated with a blend of plant oil and DME (50 wt% DME). The effect of micro-explosion on the fuel atomization by the DME was obtained, and the result showed that the combustion and exhaust characteristics of DME–plant oil



**Fig. 2** Schematic of the particle formation process (Saffaripour et al. 2014)

**Table 1** Physical and chemical properties of DME and biodiesel

Fuel parameter	DME (Park and Lee 2014)	Biodiesel (Tan et al. 2017)
Cetane number (–)	> 55	53.4
Low calorific value (MJ/kg)	27.6	39.8
Density, liquid form (kg/m <sup>3</sup> )	667	877.3
Kinematic viscosity, 20 °C (cSt)	< 0.1	6.03
Surface tension (N/m)	0.012	0.032
Latent heat of vaporization (kJ/kg)	467.13	290
Saturated vapor pressure, 25 °C (kPa)	530	–
Carbon (wt%)	52.2	76.0
Hydrogen (wt%)	13	12.3
Oxygen (wt%)	34.8	11.6
Sulfur (mg/kg)	0	48

blend engine were comparable to diesel engine. Roh et al. (2015) investigated the effect of injection mode on combustion and emission characteristics of a diesel engine fueled with DME–biodiesel blend (DME80B20). The maximum in-cylinder pressure of pilot injection mode is significantly lower than that of single injection mode. The soot emission is near zero for both single and pilot injections. Effects of DME proportion on combustion and emission of a turbocharged CI engine fueled with DME–biodiesel blend were investigated by Hou et al. (2014). The test fuels are DME100, DME70B30, DME50B50, and biodiesel. Their result showed that ignition delay, peak heat release rate, and peak in-cylinder pressure decrease with DME proportion. However, the injection timing and injection pressure which make great effect on mixture forming were not consistent throughout the experimental conditions as the pump–pipe–nozzle fuel system instead of the common rail system was used.

The advantages of diesel engine fueled with DME and biodiesel were well explained in previous limited studies focusing on spray, combustion, and conventional emissions (hydrocarbon (HC), NO<sub>x</sub>, and soot). However, there is still a gap in terms of the studies of details of particle, such as particle size distribution and polycyclic aromatic hydrocarbons

(PAHs). Ultrafine particle and PAHs have been attracting more and more attention as irregular emissions. Ultrafine particle can go deep into the human respiratory system as seen in Fig. 1 and further leads to respiratory obstruction, inflammation, and even cancer. PAHs are the precursor of particles as seen in Fig. 2 and have a strong carcinogenic effect although they only account for a very small part of engine exhaust pollutants (Saffaripour et al. 2014). Epidemiological investigation found that PAHs in urban air particles were related to the incidence and mortality of lung cancer (Bortey-Sam et al. 2015). Shi et al. (2014) measured the emissions of PM<sub>10</sub>, PM<sub>2.5</sub>, and 16 PAHs in Tianjin. The results showed that the vehicle engine occupied the largest source contributions (48.97% for PM<sub>10</sub>, 53.56% for PM<sub>2.5</sub>).

Limited research studies have concerned the particle size distribution and PAHs from diesel engine fueled with alternative fuels (DME (Li et al. 2008), DME–diesel (Liu et al. 2008), biodiesel (Lin et al. 2006; Song et al. 2011), biodiesel–diesel (Guariero et al. 2014)). Lu et al. (2012) investigated the size distribution of elemental carbon and particle-phase PAH emission from a direct injection diesel engine fueled with a waste cooking biodiesel, ultra-low sulfur diesel (ULSD, 10 ppm wt), and low sulfur diesel (LSD,

**Fig. 3** A six-cylinder turbocharged common rail DME engine**Table 2** Technical parameters of test engine

Engine type	Four-stroke turbocharged inter-cooled CIDI engine
Cylinder number	6
Bore × stroke (mm)	105 × 120
Compression ratio	18
Displacement (L)	6.32
Maximum power (kW)/speed (rpm)	155/2300
Maximum torque (N/m)/speed (rpm)	650/1600
Nozzle orifice number × diameter (mm)	7 × 0.26
Injection system	Common rail

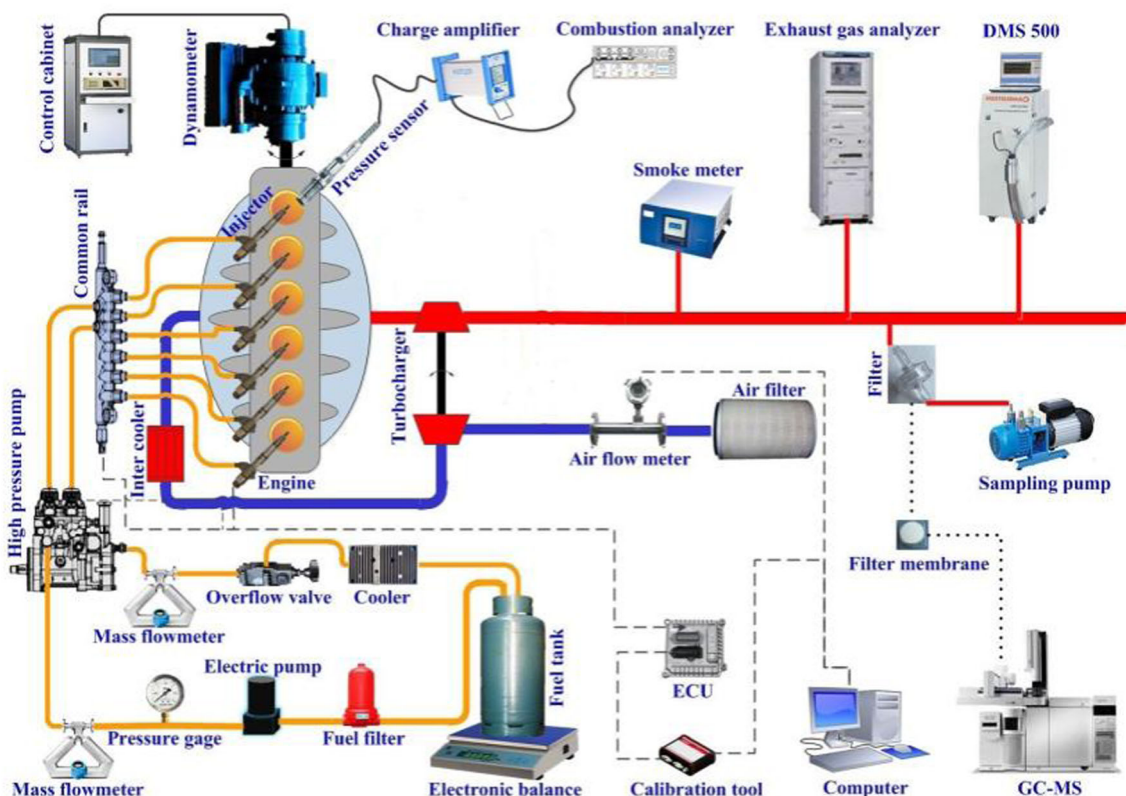


Fig. 4 Schematic of the test engine experimental setup

400 ppm wt). Biodiesel engine showed the lowest emissions of particle-phase PAHs and nuclei mode particles. Liu et al. (2008) investigated the effect of combustion mode on particle size distribution of an engine fueled with DME. The total exhaust particle number concentration for compound charge compression ignition (CCCI) combustion was slightly lower than that for homogeneous charge compression ignition (HCCI) but 20.0–29.3% higher than that for compression ignition direct injection (CIDI). Tan et al. (2017) investigated the effect of exhaust aftertreatment techniques on particle emissions from a diesel engine fueled with biodiesel–diesel blend (20% biodiesel by volume). Their study indicated the effectiveness of DOC + DPF, which could reduce the total particle number by 82.54%. Yilmaz and Davis (2016) investigated the PAHs from a diesel engine fueled with *n*-butanol and biodiesel blend. They found that most of the aromatic hydrocarbons were emitted as semi-volatile compounds.

Table 3 Test conditions of engine

Speed (rpm)	1262
Brake mean effective pressure (MPa)	0.2, 0.4, 0.6, 0.8, 1.0, 1.2
Fuel	DME, B5, B10, B15
Start of injection timing (°CA ATDC)	−4
Injection pressure (MPa)	45

Song et al. (2011) examined PAHs from a heavy-duty diesel engine fueled with cottonseed oil biodiesel. The results showed that the toxic equivalency factors (TEFs) of cottonseed oil biodiesel was half the TEFs of diesel. Borillo et al. (2018) conducted a research on the effect of SCR aftertreatment on PAH emissions from a diesel fueled with biodiesel–diesel blends. It is suggested that engine equipped with the SCR system and running with a large percentage of biodiesel could suppresses PAH emissions.

Table 4 Measurement accuracy of the parameters

Parameter	Range	Accuracy
Mass fuel consumption (kg/h)	0–20	±0.01
CO (vol%)	0–10	±0.05
HC (ppm)	0–20,000	±0.05
NO <sub>x</sub> (ppm)	0–5000	±0.05
Particle mean diameter (nm)	10–487	±0.01
Particle number concentration (/cm <sup>3</sup> )	10 <sup>2</sup> –10 <sup>7</sup>	±0.025
Speed (rpm)	0–10,000	±1
Exhaust gas temperature (°C)	0–800	±1
In-cylinder pressure (MPa)	0–25	±0.0005
Crank angle (°)		±1
Inlet gas mass flow rate (kg/h)	0–800	±0.01



Fig. 5 Fast particulate analyzer DMS500

Both DME and biodiesel are attractive alternative fuels for diesel engine. Blending DME and biodiesel could overcome their own disadvantages. Recently, more and more attention has been paid on ultrafine particle and its toxicity; however, there are only few experimental studies on performance of turbocharged common rail DME–biodiesel engine. The size distribution and toxicity of exhaust particles are still absent. Therefore, this study describes the detailed particle size distributions and PAHs of exhaust particles from a turbocharged common rail engine fueled with DME and biodiesel blends. Effects of blend ratio and engine load on formation mode of exhaust particles and particle toxicity are evaluated.

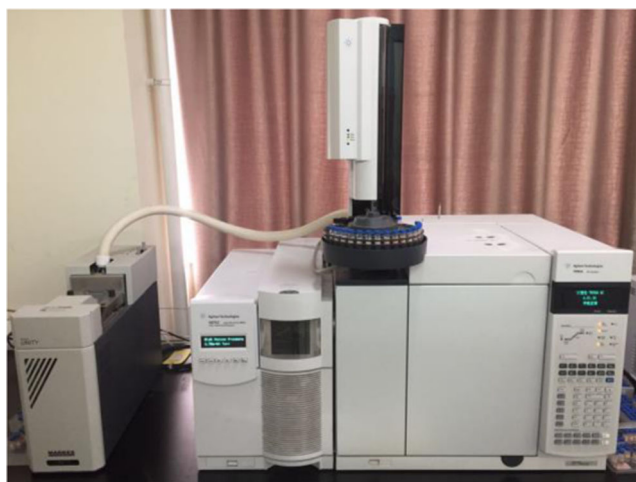


Fig. 6 Gas chromatography mass spectrometer (GC-MS)

## Experimental apparatus and method

### Test fuel and engine

The test DME–biodiesel blends are DME, B5, B10, and B15, which includes 0% biodiesel, 5% biodiesel, 10% biodiesel, and 15% biodiesel, by weight, respectively. The DME was supplied by Xinao Xinneng Energy Co., Ltd. (Zhangjiagang, Shandong Province, China). The biodiesel was derived from waste cooking oil and fulfills the standard in China (GB/T 20828-2015) (2015). The basic properties of DME and biodiesel are presented in Table 1.

A six-cylinder turbocharged common rail DME engine for test is shown in Fig. 3, with specific details in Table 2. Engine test bed is schematically shown in Fig. 4, including an electronically controlled DME–biodiesel engine, an exhaust gas recirculation system, a combustion measurement and control system, and an emission test system.

The direct injection fuel system is an electronic common rail system with modified program. The low-pressure supply pump pressurized DME or DME–biodiesel blends at 1.6 MPa to prevent vapor lock in the fuel system. In-cylinder pressure was acquired by a piezoelectric sensor (6052C, Kistler) and a charge amplifier (5018A, Kistler). Sampling frequency is 20 kHz. The pressure data of 100 consecutive cycles was sampled and recorded. The heat release rate (HRR) and the mean gas temperature were calculated using the first-law heat release model. The consumption of DME was measured by an electronic scale.

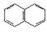
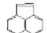
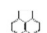

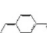



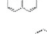
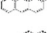
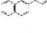
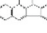

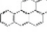

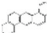
These DME–biodiesel blends were tested at six different engine loads (brake mean effective pressure (BMEP) = 0.2 MPa, 0.4 MPa, 0.6 MPa, 0.8 MPa, 1.0 MPa, and 1.2 MPa) at 1262 rpm to determine engine performance, and at three different loads (BMEP = 0.4 MPa, 0.8 MPa, and 1.2 MPa) to quantify distributions of particle size and PAHs. The test speed (1262 rpm, 55% rated speed) was chosen for which occupies the largest proportion in the 13 working conditions of the world-harmonized stationary cycle (WHSC).

To ensure reliability and stability, the maximum values of pressure rise rate, in-cylinder pressure, and cyclic fluctuation were controlled below 1 MPa/°CA, 13 MPa, and 5%, respectively. Combustion test conditions of DME–biodiesel engine are shown in Table 3, and the measurement accuracy of the parameters is listed in Table 4.

### Particle analysis

Particle size and number were measured using a Cambustion DMS500 Mk II Particle Spectrometer as seen in Fig. 5. Exhaust gas was diluted by a two-stage dilution channel before flowing into the analyzer. The first stage of the dilution channel is of the dilution ratio 5:1, and the large size particles (particle diameter > 1000 nm) were removed. The second stage is of high dilution stage with the dilution ratio ranging

**Table 5** TE of 16 common PAHs

PAH	Molecular formula	Molecular structure	TEF (Nisbet and LaGoy,1992)
Nap	C <sub>10</sub> H <sub>8</sub>		0.001
AcPy	C <sub>12</sub> H <sub>8</sub>		0.001
Acp	C <sub>12</sub> H <sub>10</sub>		0.001
Flu	C <sub>13</sub> H <sub>10</sub>		0.001
PA	C <sub>14</sub> H <sub>10</sub>		0.001
Ant	C <sub>14</sub> H <sub>10</sub>		0.01
FL	C <sub>16</sub> H <sub>10</sub>		0.001
Pyr	C <sub>16</sub> H <sub>10</sub>		0.001
BaA	C <sub>18</sub> H <sub>10</sub>		0.1
CHR	C <sub>18</sub> H <sub>12</sub>		0.01
BbF	C <sub>20</sub> H <sub>12</sub>		0.1
BkF	C <sub>20</sub> H <sub>12</sub>		0.1
BaP	C <sub>20</sub> H <sub>12</sub>		1
IND	C <sub>22</sub> H <sub>12</sub>		0.1
DBA	C <sub>22</sub> H <sub>14</sub>		1
BghiP	C <sub>22</sub> H <sub>12</sub>		0.01

from 12:1 to 500:1. To describe the particle formation mode, this paper defines that the particle diameter < 50 nm is of nucleation mode, and the particle diameter in the range of 50~1000 nm is of the accumulated mode.

### PAH collection and analysis

PAHs were analyzed using a gas chromatography mass spectrometer (GC-MS) by Agilent Technologies (model 7890-5975) as seen in Fig. 6. The GC-MS's analytical conditions were chosen according to the recommendation from EPA610 (1992) for determination of PAHs in exhaust particles. HP-5MS column (specification, 30 m × 0.25 mm × 0.25 μm) was adopted, carrier gas was hydrogen, column temperature was 300 °C, flow rate was 1.0 mL/min, and splitless injection volume was 1.0 μL.

Column temperature controlling process is as follows: (a) Set initial temperature 50 °C, hold for 1 min; (b) raise temperature to 200 °C, then hold for 2 min; and (c) raise temperature to 320 °C, then hold for 1 min. Full scan mode and selective ion detection mode were selected for mass spectrometer. Quantification of PAH components was performed by the external standard method. Firstly, the standard samples were configured into six different gradients (20 μg/mL, 40 μg/mL, 80 μg/mL, 200 μg/mL, 400 μg/mL, 800 μg/mL) by dichloromethane. Secondly, the peak area of spectrum was

calculated based on the obtained standard sample chromatogram, and the actual contents of PAHs were determined by the sample size and the PAH content of the standard sample. Finally, the standard curve of PAHs was obtained by fitting the above data.

To describe the toxicity of PAHs, TEF based on the toxicity of benzo[a]pyrene (BaP) (Nisbet and LaGoy 1992) was adopted in this study as shown in Table 5. Toxicity equivalent (TE) of particle-bound PAHs is calculated as follows:

$$TE = \sum A_i \times TEF_i \quad (1)$$

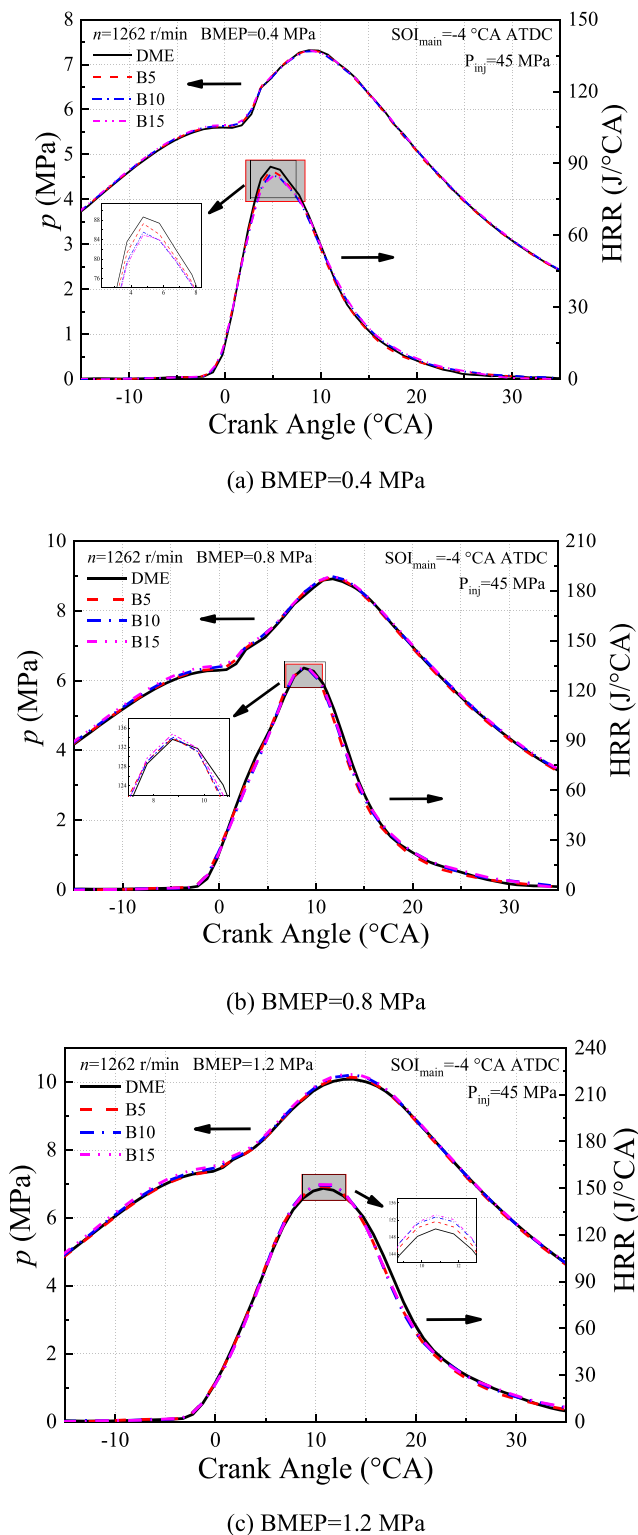
where  $A_i$  is the measured PAH emission concentration.

## Results and discussion

### Engine performance

#### Combustion characteristics

Effects of biodiesel proportion and engine load on cylinder pressure and heat release rate of cylinder 6 at 1262 rpm are shown in Fig. 7. The curves of in-cylinder pressure and HRR of various fuels are of the same shape. In this study, the four blends have excellent atomization characteristics (high



**Fig. 7** Effect of biodiesel proportion and BMEP on in-cylinder pressure and heat release rate. **a** BMEP = 0.4 MPa. **b** BMEP = 0.8 MPa. **c** BMEP = 1.2 MPa

saturated vapor pressure) and high cetane number, as the DME accounts for the majority ( $\geq 85\%$ ) of the blends. What is more, due to the higher intake temperature and intake

pressure of turbocharged engine, the ignition delay period is shorter than naturally aspirated diesel engine. Thus, the combustion that this study presents is the diffusion-dominated combustion mode and one-stage heat release law, with small premixed combustion. The HRR of an electronically controlled turbocharged common rail DME–biodiesel engine is quite different from previous results that both premixed and diffusion combustions significantly occur in the naturally aspirated DME–biodiesel engine with in-line pump (Wang et al. 2011).

Figure 8 shows the effects of EGR rate on ignition delay and combustion duration in cylinder 6. Ignition delay almost linearly increases with the engine load, as the residence time for the  $O_2$ –fuel interaction increases at higher loads due to the higher cycle fuel injection quantity. The effects of biodiesel proportion on the ignition delay are complex, and B5 shows the shortest ignition delay. The following four factors could explain the results:

- The cetane number of biodiesel is slightly lower than that of DME, and the chemical ignition delay time is slightly longer than that of DME.
- The high viscosity, surface tension, and distillation range of biodiesel lead to poor atomization performance.
- The calorific value of biodiesel is more than 40% higher than that of DME, and the modulus of elasticity is larger than that of DME, resulting in the much shorter-duration fuel injection of biodiesel compared with DME.
- By adding a small amount of biodiesel in DME, the spray cone angle decreases, while the spray penetration distance and the spray area increase (Kim et al. 2010) which promote the fuel– $O_2$  fast mixing.

In this study, effects of (c) and (d) advancing the ignition delay are slightly stronger than those of (a) and (b), and the ignition delay of B5 is the shortest, followed by DME. With the increase of the biodiesel proportion up to 10%, the effect of (b) increases, and the ignition delay time is extended as seen in Fig. 8 a.

Although blends with higher DME proportion require more fuels to be injected into the cylinder due to the lower heating value, which promotes the extension of combustion duration. The combustion durations of B5 and DME are relatively short as seen in Fig. 8 b owing to the high volatility, high oxygen content, and high cetane number. High volatility promotes the atomization and mixture formation, high oxygen content is available for promoting combustion especially the diffusive combustion (Ren et al. 2008), and high cetane number improves the chemical reaction rate, all these are conducive to shorten the combustion duration time. Moreover, analysis of ignition kinetics showed that the peak mole fractions of H and OH radicals promoting the ignition increase with an increasing

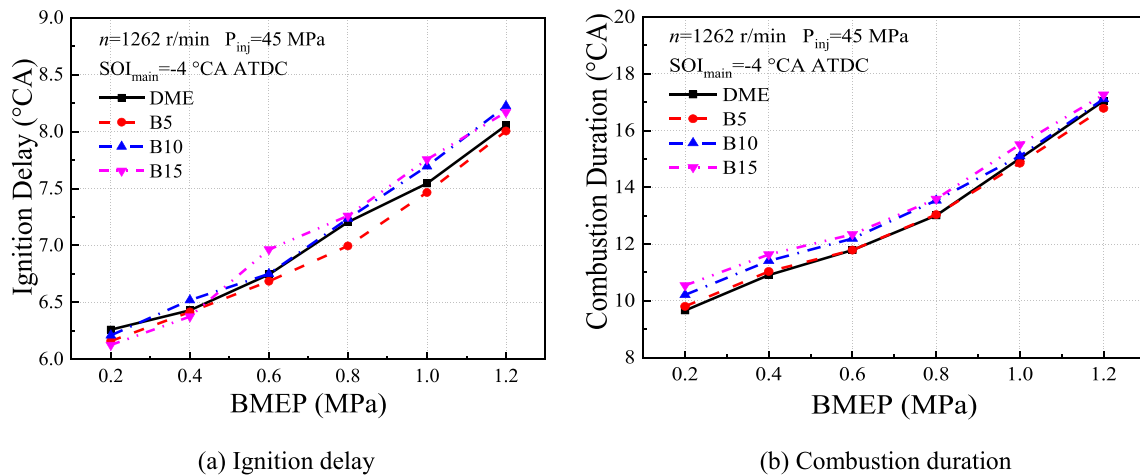


Fig. 8 Effect of biodiesel proportion on ignition delay and combustion duration. a Ignition delay. b Combustion duration

DME blending ratio, as CH<sub>3</sub> and CH<sub>2</sub>O are the major products during the oxidation of DME (Jiang et al. 2013; Hu et al. 2012).

**Fuel consumption and exhaust gas temperature**

Effects of biodiesel proportion and engine load on equivalent brake-specific fuel consumption (EBSFC) and brake thermal efficiency (BTE) are shown in Figs. 9 and 10, respectively. The EBSFC is calculated by converting the DME–biodiesel consumption to that of the diesel.

$$EBSFC = BSFC_{Blend} \times \frac{H_{u,Blend}}{H_{u,Diesel}} \tag{1}$$

where BSFC<sub>Blend</sub> is the effective fuel consumption rate of DME–biodiesel blends (g/kWh), H<sub>u,Blend</sub> is the low calorific value of blends (MJ/kg), and H<sub>u,Diesel</sub> is the low calorific value of diesel (MJ/kg).

The variation of EBSFC with biodiesel proportion in Fig. 9 shows the similar trend with the combustion duration in Fig. 8

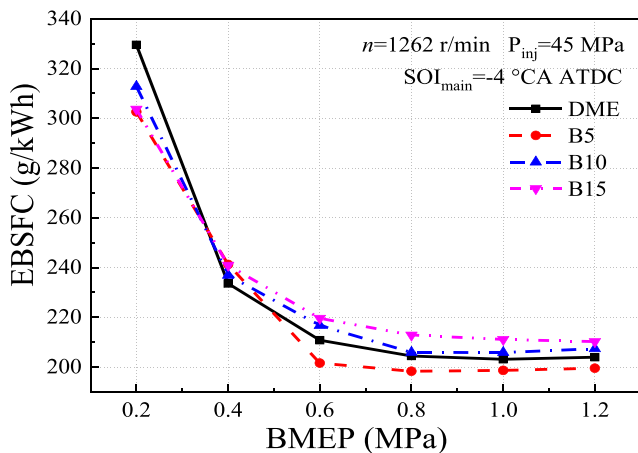


Fig. 9 Effect of biodiesel proportion and BMEP on EBSFC

b. B5 shows the shortest combustion duration and the lowest EBSFC, followed by the DME, and B15 shows the longest combustion and the highest EBSFC. An increase in combustion duration leads to reductions of volumetric efficiency and thermal efficiency. With the increase of engine load, the BTE increases first and then decreases as shown in Fig. 10. The maximum BTE of the DME and blends is 41.3%, 42.6%, 41.0%, and 39.7%, respectively, near the engine load of BMEP = 0.8 MPa. Extending the combustion duration can delay the combustion end-point and finally increase the exhaust thermal loss and exhaust gas temperature as shown in Fig. 11.

**Particle number size distribution**

Particle number size distribution and its cumulative mode with varied biodiesel proportions and engine loads are shown in Fig. 12. The temperature is the major determinant of particle formation and oxidation. Figure 13 gives the effects of biodiesel proportion and engine load on the

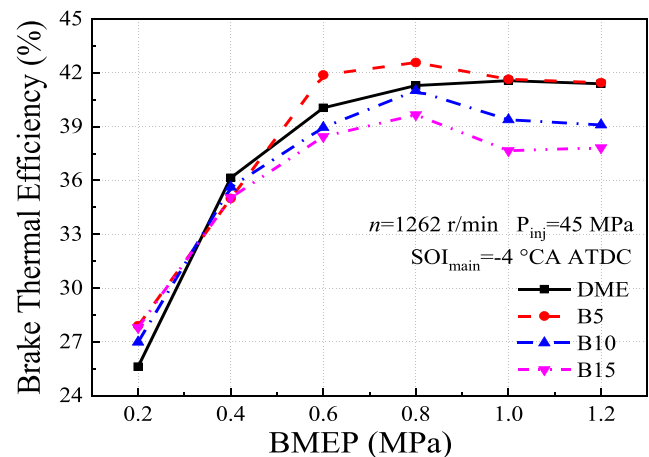
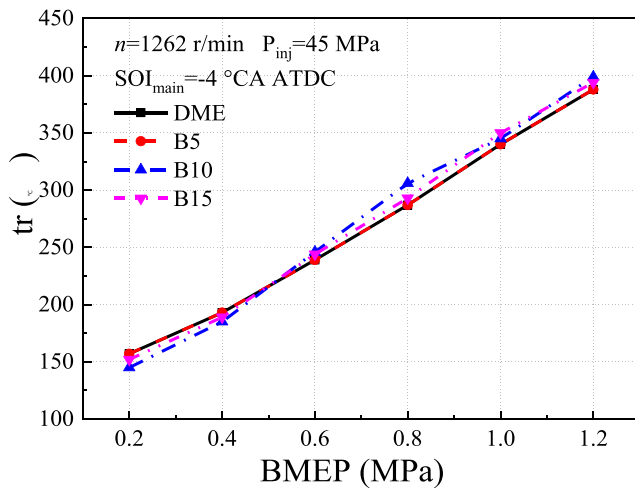


Fig. 10 Effect of biodiesel proportion and BMEP on brake thermal efficiency





**Fig. 11** Effect of biodiesel proportion and BMEP on temperature of exhaust gas

in-cylinder temperature versus crank angle. The particle size distributions of DME–biodiesel show a bimodal structure with the nucleation mode (peak at 10–30 nm) and the accumulation mode (peak at 200–400 nm). The nucleation mode particles are the secondary particles formed by the distribution of volatile or semi-volatile components such as sulfuric acid or HC to form nuclei or condensation. The accumulation mode particles are mainly formed by the accumulation of primary carbon particles (particle size of about 2 nm) condensed with part of HC.

Figure 12 shows that the nucleation mode particles of DME–biodiesel engine occupy the main composition of particle emissions. The accumulation mode particle number of DME–biodiesel engine is much lower than that of diesel engine measured by Li et al. (2008). This is attributed to the higher oxygen level of the blends and the characteristic of having no C–C bond of DME (Wang et al. 2012).

Engine fueled with pure DME still exhausts some accumulation mode particles as seen in Fig. 12. This possibly correlates with incomplete combustion of lubricating oil. Hilden and Mayer (1984) showed that the incomplete lubricating oil represented about 25% of particles emitted from diesel engine in terms of mass concentration. What is more, for pure DME, anti-abrasion addition is essential to avoid the abrasion and leakage as viscosity of DME is much lower than those of diesel. The incomplete combustion of anti-abrasion addition is another factor of particle formation.

At low load (BMEP = 0.4 MPa), the particles of the four blends are mainly in the form of nucleation mode as seen in Fig. 12 a. The concentration of nucleation mode of DME, B5, B10, and B15 accounts for 99.95%, 95.22%, 97.52%, and 99.95% of the total concentration, respectively. The accumulation mode particles are very small, because most of the blends are DME which is conducive to excellent atomization

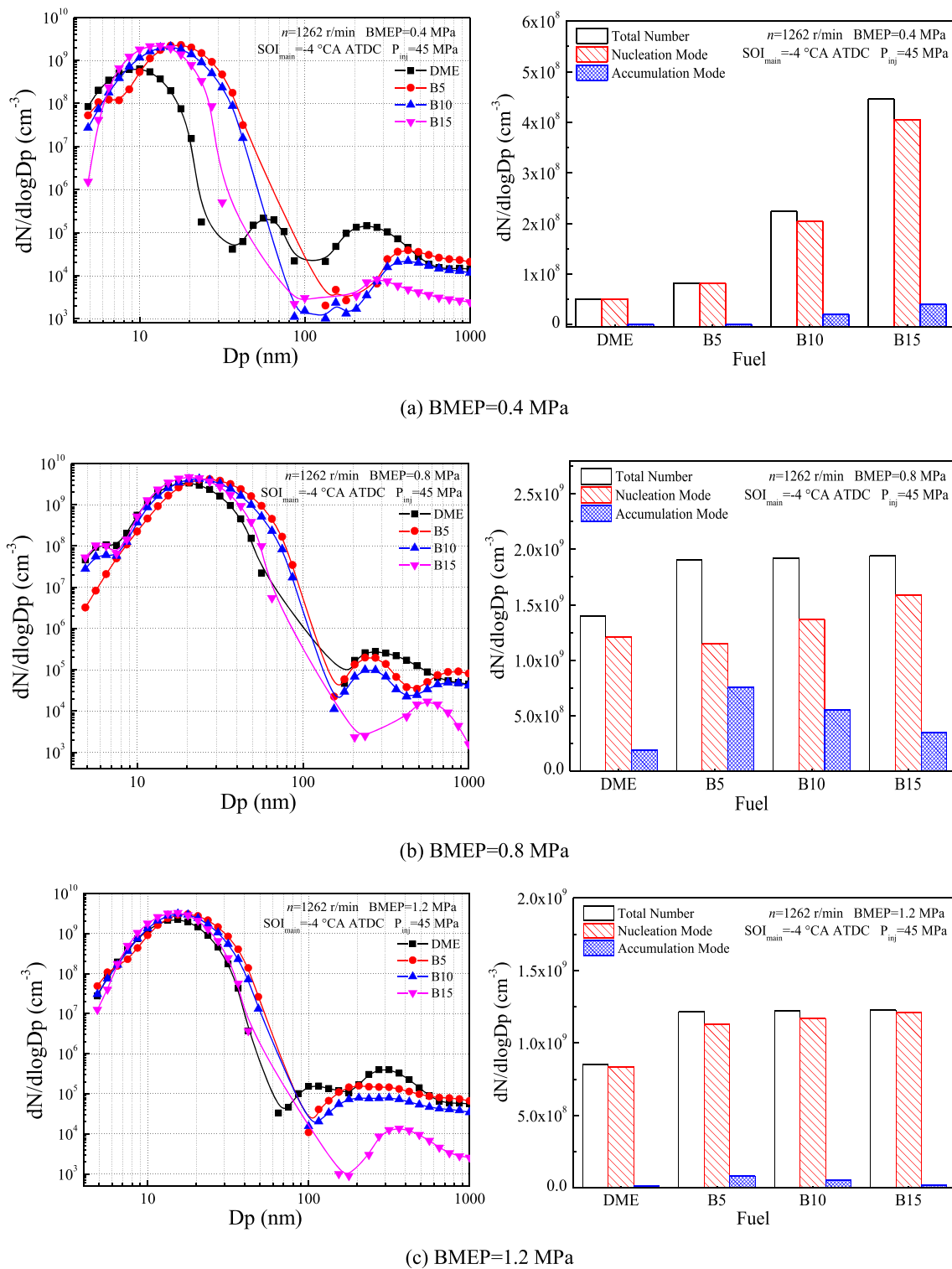
and complete combustion. Meanwhile, less cycle fuel injection at lower load also promotes finer fuel–air mixture formation and shorter combustion duration, which further suppresses the large particles during the combustion process. Compared to pure DME, increased viscosity and lower volatility of DME–biodiesel blend cause difficult atomization fuel, uneven fuel–O<sub>2</sub> mixing, inadequate combustion, and a further increase in total particle number, peak of particle number concentration, and particle size corresponding to the peak of particle number concentration as shown in Fig. 12 a. Besides, the oxygen content in biodiesel molecule is lower than that in DME, and biodiesel addition is not conducive to the oxidation of the nucleation mode particles (Ballesteros et al. 2010).

In this study, particle emission at low load is significantly lower than that at intermediate and high loads, which is completely different from the results of Lu et al. (2012) and Li et al. (2008) that engine fueled with biodiesel or DME at low load exhausts the same level particles as at intermediate and high loads, as can be seen in Fig. 14. The low injection pressure of in-line pump at low load is to blame for causing the results. Instead of the in-line pump injection system used by Lu et al. (2012) and Li et al. (2008), fuel injection type of this study is a common rail injection system which keeps the fuel injection pressure independent with cycle fuel injection volume. At low load, the combustion temperature is low as seen in Fig. 13 a while the oxygen is rich, suppressing the formation of particle emissions.

At intermediate load (BMEP = 0.8 MPa), particle sizes corresponding to the peaks of particle number concentration and particle numbers of both nucleation mode and accumulation mode are larger than those of at low load, while the effect of biodiesel proportion is weakened as shown in Fig. 12 b. With the increase of load, the cycle fuel injection volume and the combustion temperature increase as seen in Fig. 13 b, and the local hypoxia occurs. Fuels are more likely to crack at high temperatures to form soot precursors, such as CH<sub>2</sub> and C<sub>2</sub>H<sub>4</sub>, and then continue to dehydrogenate to form soot nuclei. Some of the soot nuclei further form accumulation mode particles after adsorbing unburned HC and sulfate. Moreover, the increase of fuel would increase the concentration of unburned HC near the wall of combustion chamber. These volatile components would form nucleation mode particles after being cooled in the exhaust pipe.

Further increasing BMEP by up to 1.2 MPa, the effect of biodiesel proportion on particle size distribution is further weakened as shown in Fig. 12 c. High temperature during the expansion stroke is beneficial for oxidative dehydrogenation of fuel, decrease of particle size, and reduction of particle number, especially reduction of accumulation mode particle number.

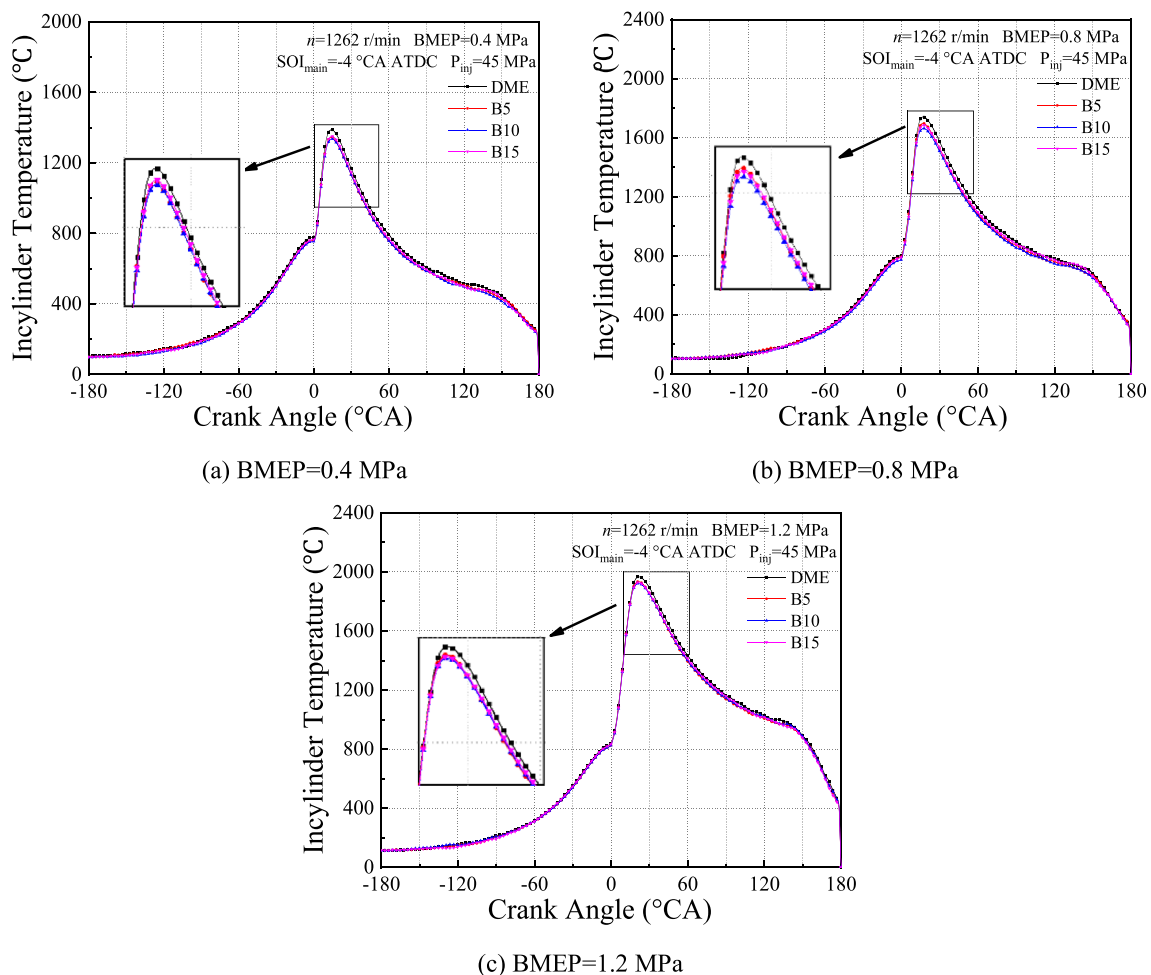
Accumulation mode particles show a non-monotonic trend with biodiesel proportion in the intermediate and high loads as seen Fig. 12 b and c. Since DME is smoke-free combustion, its soot is lower than that of DME–biodiesel blend. With the



**Fig. 12** Size distribution and cumulative mode of particles. **a** BMEP = 0.4 MPa. **b** BMEP = 0.8 MPa. **c** BMEP = 1.2 MPa

increase of biodiesel (from 5 to 15%), the injection duration is decreased as the heat value of the blend increases, while the ignition delay is increased as seen in Fig. 8, which is conducive to the reduction of diffusion combustion phase and an increase in the temperature during the expansion stroke as

seen in Fig. 13. A shorter diffusion combustion phase suppresses the particle formation as the PM originates from the fuel-rich side of the reaction zone in the diffusion-controlled combustion phase (Stone 2012), and a higher temperature during the expansion stroke promotes the soot oxidation.



**Fig. 13** Effect of biodiesel proportion and BMEP on in-cylinder temperature. **a** BMEP = 0.4 MPa. **b** BMEP = 0.8 MPa. **c** BMEP = 1.2 MPa

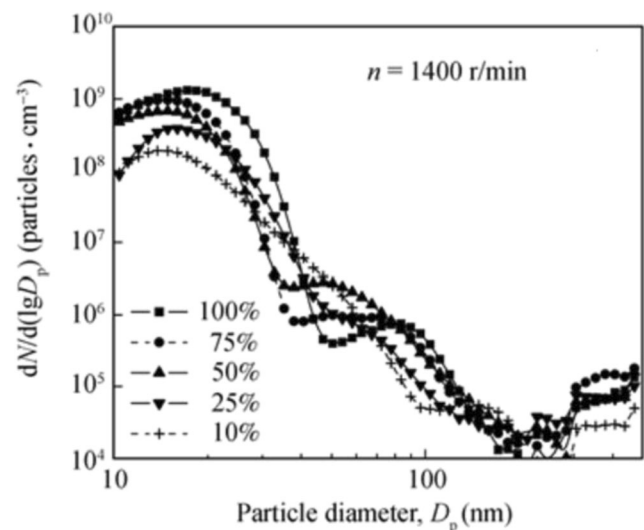
In general, the results indicate that the addition of biodiesel (biodiesel proportion  $\leq 15\%$ wt) in DME can release the DME engine from abrasion and leakage, but no obvious increase in particle emission.

### PAHs and toxicity

Both DME and biodiesel can effectively reduce the emissions of PAHs, and the emissions of the total particle-associated PAHs decrease by 30% at least on both low and high engine loads, compared with fossil diesel (Lu et al. 2012). It could be attributed to the oxygen in DME and biodiesel which induces a more complete combustion (Ballesteros et al. 2010). Two sources are associated to PAH emissions, namely survival of the PAHs originally present in fuel or lubricant oil, and combustion reaction in which PAHs are formed through pyro-synthesis of the fuel fragments (Collier et al. 1995).

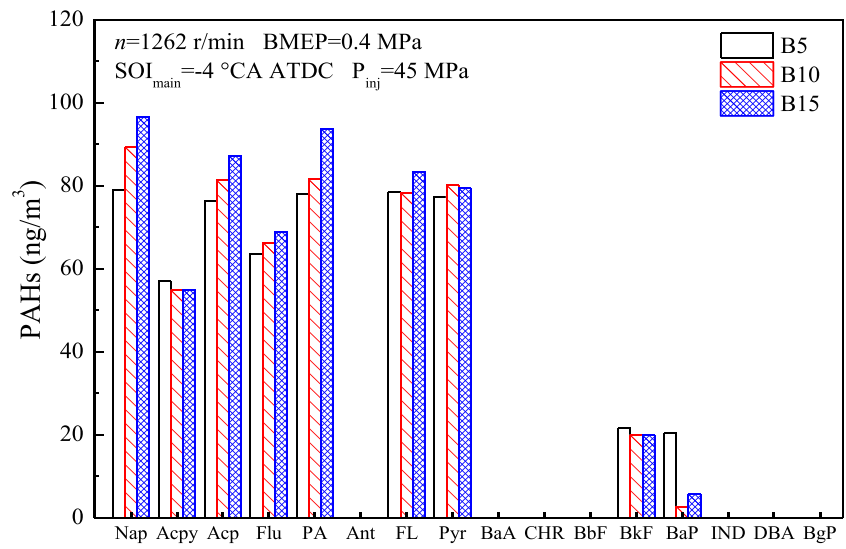
Figures 15 and 16 show the effect of different biodiesel proportions (B5 and B15) and engine loads (BMEP = 0.4 MPa and 0.8 MPa) on distribution of PAHs and total PAH emissions. No argon (Ant), benzo[a]pyrene (BaA),

hydrazine (CHR), benzo[b]fluoranthene (BbF), indenopyrene (IND), dibenz[a,h]anthracene (DBA), and benzo[g,h,i]perylene (BgP) were detected. Concentration of the most toxic PAH

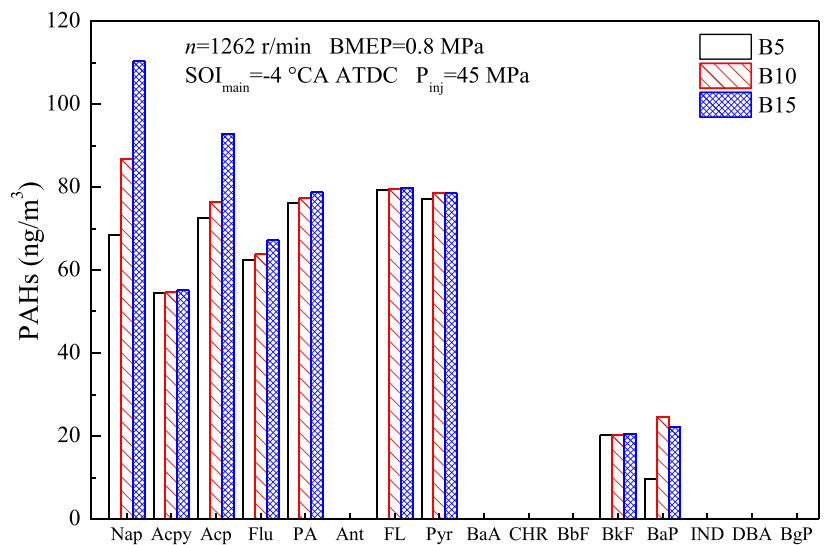


**Fig. 14** Influence of engine load on the exhaust particle size distribution of the DME engine (Li et al. 2008)

**Fig. 15** Detailed components of PAHs. **a** BMEP = 0.4 MPa. **b** BMEP = 0.8 MPa



(a) BMEP=0.4 Mpa



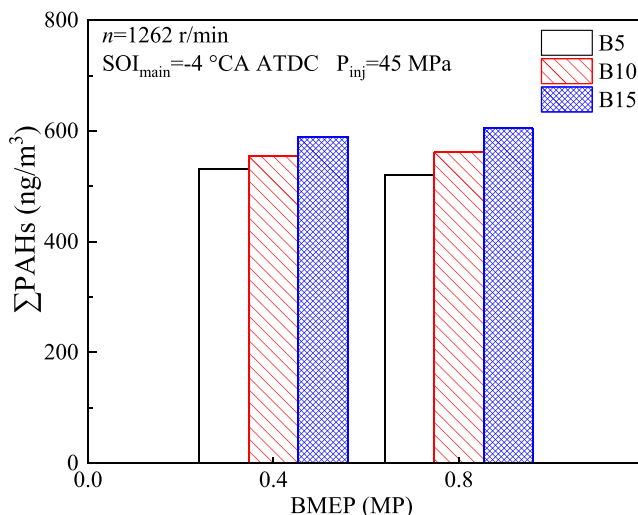
(b) BMEP=0.8 Mpa

(benzo(a)pyrene (BaP)) is very low, less than 30 ng/m<sup>3</sup>. With the increase of biodiesel proportion, concentration of naphthalene (Nap), acenaphthylene (Acp), fluorene (flu), phenanthrene (PA), and fluoranthene (FL) increases, and total PAH emissions increase.

Figure 17 shows the effect of biodiesel proportion and engine load on concentration of PAHs in each benzene ring, and it shows that there is no six-ring PAH. Among the detected PAHs, three- and four-ring PAHs are the predominant components and five-ring PAHs are the lowest. With the increase of biodiesel proportion, concentrations of two-, three-, and four-ring PAHs increase. As can be seen in Fig. 17, low molecular weight PAHs occupy a larger mass fraction in the total PAHs at both low and intermediate engine loads, while low

molecular weight PAHs are mainly derived from the unburned fuel (Marr et al. 1999).

Figure 18 shows the effects of biodiesel proportion and engine load on the TE of particles. At low load (BMEP = 0.4 MPa), the toxicity equivalent of particles decreases first and then increases with an increase in biodiesel proportion. While at intermediate load (BMEP = 0.8 MPa), the toxicity equivalent of particles increases first and then decreases with an increase in biodiesel proportion. For B10 and B15, engine operated at higher load exhausts particles with higher toxicity, while it is on the contrary for B5. In this study, engine fueled with B10 at low load exhausts the lowest TE of particles, while B10 at intermediate load exhausts the highest TE of particles. In general,



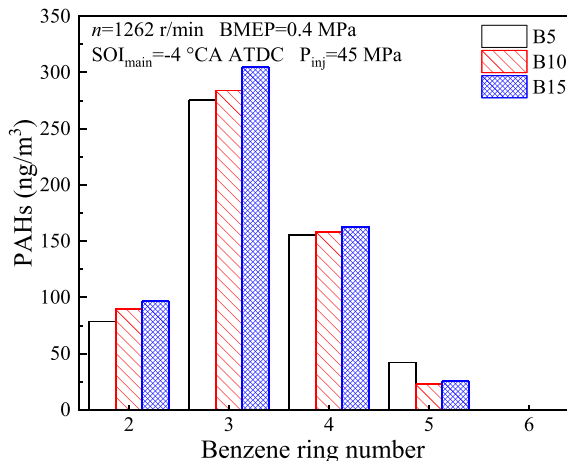
**Fig. 16** Total PAH emissions

the addition of a small amount of biodiesel in DME would not increase the risk of particle toxicity.

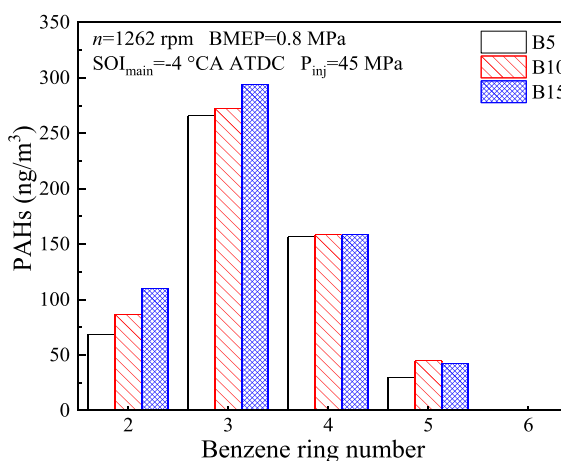
## Conclusions

The experimental study was conducted on a turbocharged common rail compression ignition engine fueled with DME and DME–biodiesel blends which is DME, B5, B10, and B15. Effects of biodiesel proportion on engine combustion, performance, particle number distribution, and particle toxicity were obtained. The following conclusions were reached:

- (1) The combustion characteristics show a non-monotonic trend with biodiesel proportion as the quite difference of chemical and physical properties between DME and biodiesel. B5 shows the shortest ignition delay and combustion duration, followed by DME, and B15 showing the longest.

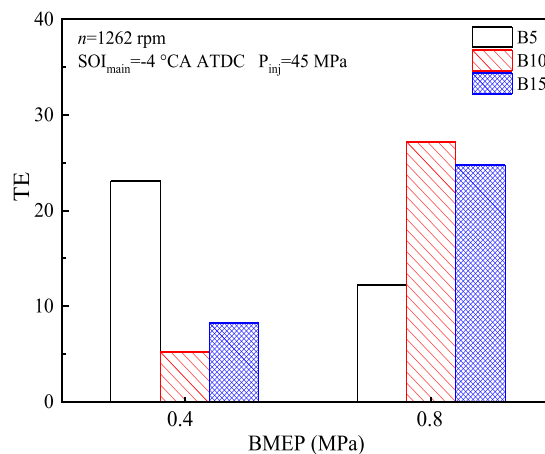


(a) BMEP=0.4 Mpa



(b) BMEP=0.8 Mpa

**Fig. 17** PAH emissions with various benzene rings. **a** BMEP = 0.4 MPa. **b** BMEP = 0.8 MPa



**Fig. 18** Total toxicity equivalent of particles

- (2) With an increase in engine load, the BTE increases first and then decreases, and the maximum BTE levels of the DME and blends were achieved at medium-to-high load. The BTE of B5 is the highest, followed by DME, and B15 showing the lowest, which shows the same trend with combustion duration.
- (3) Exhaust particles from engine fueled with DME, B5, B10, and B15 are mainly in the form of nucleation mode (particle diameter < 50 nm), especially at low load (BMEP = 0.4 MPa) and high load (BMEP = 1.2 MPa), and the number of nucleation mode particles accounts for more than 95%.
- (4) For all loads, the particle size distributions of DME–biodiesel blends show a bimodal structure with the nucleation mode (peak at 10–30 nm) and the accumulation mode (peak at 200–400 nm). The addition of biodiesel results in an increase in total particle number, peak of particle number concentration, and particle size corresponding to the peak of particle number concentration. The effect of biodiesel proportion on particle size distribution is weakened by increasing engine load.

- (5) No six-ring PAH forms when engine is fueled with B5, B10, and B15, and three- and four-aromatic ring PAHs occupy a larger mass fraction in the total PAH. For small additions of biodiesel, there was little change in the PAH emissions. Toxicity equivalent (TE) of particle at low load is lower than that of particle at intermediate load. Engine fueled with B10 exhausts the lowest TE of particle at low load, but the highest TE of particle at intermediate load.
- (6) The addition of a moderate amount of biodiesel (biodiesel mass proportion  $\leq 15\%$ ) in DME releases the DME engine from abrasion and leakage, but no increase in the risk of particle toxicity.

**Funding information** This project was supported by the National Key R&D Program of China (2017YFE0130800), Science Technology Department of Zhejiang Province (Grant No. GG19E060001), National Natural Science Foundation of China (Grant Nos. 91441124 and 91741122), and China Postdoctoral Science Foundation (Grant No. 2018 M642014).

## References

- Ballesteros R, Hernandez JJ, Lyons LL (2010) An experimental study of the influence of biofuel origin on particle-associated PAH emissions. *Atmos Environ* 44:930–938
- Benajes J, Novella R, Pastor JM et al (2018) Computational optimization of the combustion system of a heavy duty direct injection diesel engine operating with dimethyl-ether. *Fuel* 218:127–139
- Borillo GC, Tadano YS, Afl G et al (2018) Polycyclic aromatic hydrocarbons (PAHs) and nitrated analogs associated to particulate matter emission from a Euro V-SCR engine fuelled with diesel/biodiesel blends. *Sci Total Environ* 644:675
- Bortey-Sam N, Ikenaka Y, Akoto O, Nakayama SM, Yohannes YB, Baidoo E, Mizukawa H, Ishizuka M (2015) Levels, potential sources and human health risk of polycyclic aromatic hydrocarbons (PAHs) in particulate matter (PM 10) in Kumasi, Ghana. *Environ Sci Pollut Res* 22(13):9658–9667
- Cipolat D. (2007) The Effect of fuel characteristics on the fuel injection process in a CI engine fuelled on diesel and DME, SAE Technical Paper 2007;2007-24-0119
- Cipolat D, Bhana N (2009) Fuelling of a compression ignition engine on ethanol with DME as ignition promoter: effect of injector configuration. *Fuel Process Technol* 90(9):1107–1113
- Collier A, Rhead M, Trier C, Bell M (1995) Polycyclic aromatic compound profiles from a light-duty direct-injection diesel engine. *Fuel* 74:362–367
- Di Y, Cheung CS, Huang Z (2009) Comparison of the effect of biodiesel-diesel and ethanol-diesel on the gaseous emission of a direct-injection diesel engine. *Atmos Environ* 43(5):455–465
- Geng P, Tan Q, Zhang C, Wei L, He X, Cao E, Jiang K (2016) Experimental investigation on NO<sub>x</sub> and green house gas emissions from a marine auxiliary diesel engine using ultralow sulfur light fuel. *Sci Total Environ* 572:467–475
- Ghadikolaei MA, Cheung CS, Yung KF (2018) Study of combustion, performance and emissions of diesel engine fueled with diesel/biodiesel/alcohol blends having the same oxygen concentration. *Energy* 157:258–269
- Guariero ALN, Santos JVDS, Eiguren-Fernandez A et al (2014) Redox activity and PAH content in size-classified nanoparticles emitted by a diesel engine fuelled with biodiesel and diesel blends. *Fuel* 116(1):490–497
- Hilden DL, Mayer WJ (1984) The contribution of engine oil to particulate exhaust emissions from light-duty, diesel-powered vehicles. SAE Paper 841395
- Hou J, Wen Z, Jiang Z et al (2014) Study on combustion and emissions of a turbocharged compression ignition engine fueled with dimethyl ether and biodiesel blends. *J Energy Inst* 87(2):102–113
- Hu EJ, Jiang X, Huang ZH et al (2012) Experimental and kinetic studies on ignition delay times of dimethyl ether/n-butane/O<sub>2</sub>/Ar mixtures. *Energy Fuel* 27(1):530–536
- Hyun G, Oguma M (2002) Spray and exhaust emission characteristics of a biodiesel engine operating with the blend of plant oil and DME. SAE Technical Paper Series 2002;2002-01-0864
- Jiang X, Zhang YJ, Man XJ et al (2013) Shock tube measurements and kinetic study on ignition delay times of lean DME/n-butane blends at elevated pressures. *Energy Fuels* 27(10):6238–6246
- Kim HJ, Park SH, Lee CS (2010) A study on the macroscopic spray behavior and atomization characteristics of biodiesel and dimethyl ether sprays under increased ambient pressure. *Fuel Process Technol* 91(3):354–363
- Lamani VT, Yadav AK, Narayanappa KG (2017) Influence of low-temperature combustion and dimethyl ether-diesel blends on performance, combustion, and emission characteristics of common rail diesel engine: a CFD study. *Environ Sci Pollut Res* 24(18):15500–15509
- Li XL, Huang Z, Wang JS et al (2008) Characteristics of ultrafine particles emitted from a dimethyl ether (DME) engine. *Chin Sci Bull* 53(2):304–312
- Lin Y, Lee et al (2006) Comparison of PAH and regulated harmful matter emissions from biodiesel blends and paraffinic fuel blends on engine accumulated mileage test. *Fuel* 85(17):2516–2523
- Liu W, Qiao X, Wang J et al (2008) Effects of combustion mode on exhaust particle size distribution produced by an engine fueled by dimethyl ether (DME). *Energy Fuel* 22(6):3838–3843
- Lu T, Huang Z, Cheung CS, Ma J (2012) Size distribution of EC, OC and particle-phase PAHs emissions from a diesel engine fueled with three fuels. *Sci Total Environ* 438:33–41
- Marr LC, Kirchstetter TW, Harley RA, Miguel AH, Hering SV (1999) Characterization of polycyclic aromatic hydrocarbons in motor vehicles fuels and exhaust emissions. *Environ Sci Technol* 33:3091–3099
- Musthafa MM, Kumar TA, Mohanraj T et al (2018) A comparative study on performance, combustion and emission characteristics of diesel engine fueled by biodiesel blends with and without an additive. *Fuel* 225:343–348
- Nisbet IC, Lagoy PK (1992) Toxic equivalency factors (TEFs) for polycyclic aromatic hydrocarbons (PAHs). *Regulatory Toxicol Pharmacol* 16(3):290–300
- Park SH, Lee CS (2014) Applicability of dimethyl ether (DME) in a compression ignition engine as an alternative fuel. *Energy Convers Manag* 86:848–863
- Peng G, Cao E, Tan Q et al (2017) Effects of alternative fuels on the combustion characteristics and emission products from diesel engines: a review. *Renew Sustain Energy Rev* 71:523–534
- Ren Y, Huang ZH, Miao HY et al (2008) Combustion and emissions of a DI diesel engine fueled with diesel-oxygenate. *Fuel* 87(12):2691–2697
- Roh HG, Lee D, Chang SL (2015) Impact of DME-biodiesel, diesel-biodiesel and diesel fuels on the combustion and emission reduction characteristics of a CI engine according to pilot and single injection strategies. *J Energy Inst* 88(4):376–385
- Saffaripour M, Veshkini A, Kholghy M et al (2014) Experimental investigation and detailed modeling of soot aggregate formation and size distribution in laminar coflow diffusion flames of Jet A-1, a synthetic kerosene, and n-decane. *Combustion & Flame* 161(3):848–863

- Şen M, Emiroğlu AO, Keskin A (2018) Production of biodiesel from broiler chicken rendering fat and investigation of its effects on combustion, performance, and emissions of a diesel engine. *Energy Fuel* 32(4):5209–5217
- Shi GL, Liu GR, Tian YZ et al (2014) Chemical characteristic and toxicity assessment of particle associated PAHs for the short-term anthropogenic activity event: during the Chinese New Year's Festival in 2013. *Science of the Total Environment* 482–483:8–14
- Song J, Huang Z, Qiao X et al (2004) Performance of a controllable premixed combustion engine fueled with dimethyl ether. *Energy Conversion & Management* 45(13):2223–2232
- Song WW, He KB, Wang JX, Wang XT, Shi XY, Yu C, Chen WM, Zheng L (2011) Emissions of EC, OC, and PAHs from cottonseed oil biodiesel in a heavy-duty diesel engine. *Environmental Science & Technology* 45(15):6683–6689
- Soni DK, Gupta R (2017) Application of nano emulsion method in a methanol powered diesel engine. *Energy* 126:638–648
- Stone R. *Introduction to internal combustion engines*, 4th edition editio. London: Palgrave Macmillan, 2012
- Tan PQ, Zhong YM, Hu ZY et al (2017) Size distributions, PAHs and inorganic ions of exhaust particles from a heavy duty diesel engine using B20 biodiesel with different exhaust aftertreatments. *Energy* 141(15):898–906
- USA EPA. Polynuclear aromatic hydrocarbons. EPA 610 1992;441–454
- Wang Y, Li G, Zhu W et al (2008) Study on the application of DME/diesel blends in a diesel engine. *Fuel Process Technol* 89(12):1272–1280
- Wang Z, Qiao X, Hou J et al (2011) Combustion and emission characteristics of a diesel engine fuelled with biodiesel/dimethyl ether blends. *Proceedings of the Institution of Mechanical Engineers, Part D: Journal of Automobile Engineering* 225(12):1683–1691
- Wang XG, Cheung CS, Di YG et al (2012) Diesel engine gaseous and particle emissions fueled with diesel-oxygenate blends. *Fuel* 94: 317–323
- Yilmaz N, Davis SM (2016) Polycyclic aromatic hydrocarbon (PAH) formation in a diesel engine fueled with diesel, biodiesel and biodiesel/n-butanol blends. *Fuel* 181:729–740

**Publisher's note** Springer Nature remains neutral with regard to jurisdictional claims in published maps and institutional affiliations.